Electron emission and energy loss in grazing collisions of protons with insulator surfaces

M. S. Gravielle,[1] I. Aldazabal,[2] A. Arnau,[2,3] V. H. Ponce,[4,5] J. E. Miraglia,[1] F. Aumayr,[6] S. Lederer,[7] and H. Winter[7]
[1]*Instituto de Astronomía y Física del Espacio, Consejo Nacional de Investigaciones Científicas y Técnicas, and Departamento de Física, Facultad de Ciencias Exactas y Naturales, Universidad de Buenos Aires, Buenos Aires, Argentina*
[2]*Departamento de Física de Materiales, Facultad de Química, UPV/EHU, San Sebastian, Spain*
[3]*CentroMixto CSIC-UPV/EHU, San Sebastian, Spain*
[4]*Centro Atómico Bariloche, San Carlos de Bariloche, Argentina*
[5]*Donostia International Physics Center (DIPC), San Sebastian, Spain*
[6]*Institut für Allgemeine Physik der TU Wien, Wiedner Haupstrasse 8-10, A-1040 Wien, Austria*
[7]*Institut für Physik, Humboldt Universität zu Berlin, Brook-Taylor-Strasse 6, D-12489 Berlin-Adlershof, Germany*
(Received 2 January 2007; revised manuscript received 7 May 2007; published 31 July 2007)

Electron emission from LiF, KCl, and KI crystal surfaces during grazing collisions of swift protons is studied using a first-order distorted-wave formalism. Owing to the localized character of the electronic structure of these surfaces, we propose a model that allows us to describe the process as a sequence of atomic transitions from different target ions. Experimental results are presented for electron emission from LiF and KI and energy loss from KI surfaces. Calculations show reasonable agreement with these experimental data. The role played by the charge of the incident particle is also investigated.

DOI: 10.1103/PhysRevA.76.012904 PACS number(s): 34.50.Dy, 34.50.Fa, 34.50.Bw

I. INTRODUCTION

The interaction during grazing scattering of fast ions from insulator surfaces comprises two interesting features: the localized character of the electronic structure of the surface and the geometry of the collision that favors large electron yields [1,2]. In this work we investigate electron emission produced during grazing collisions of fast protons with ionic crystals such as LiF, KCl, and KI. These materials are typical broad band-gap insulators with a narrow valence band, which indicates that the valence electrons retain essential parts of their atomic character.

At high impact energies, protons move along the trajectory mainly as bare ions. Therefore, ejected electrons essentially originate from direct ionization of the surface. To describe this process we employ a theoretical model that makes use of the local character retained by the valence electrons, representing the electronic transitions induced by the projectile along its path as a succession of single collisions with the surface ions [3]. In this model, target ionization probabilities associated with binary encounters are evaluated with the continuum-distorted-wave eikonal-initial-state (CDW-EIS) approximation, which is a distorted-wave method successfully used in the field of ion-atom collisions [4]. The classical trajectory of the incident ion is described by means of a punctual model [5] that considers the individual interactions of the projectile with the solid ions placed at the sites of the crystal lattice.

For the different targets we present calculations of the electron emission probability as a function of the incidence angle and discuss the influence of the electronic structure of the medium. In the cases of LiF and KI, theoretical results are compared with measurements of electron emission yields for grazing scattering of hydrogen atoms.

In addition, we study the energy loss of projectiles during grazing scattering. Experimental data for the energy loss of H^0 colliding with a KI(001) surface are shown and compared with values obtained from the theoretical model. The role played by the charge state of the projectile is analyzed. A small fraction of H^0 gives an important contribution around the convoy peak that appears in electron emission spectra measured in the forward direction [6], but this mechanism of projectile ionization is negligible compared to the total electron emission yield and energy loss.

The theoretical formalism is summarized in Sec. II, and the experimental method and setup are described in Sec. III. In Sec. IV we discuss results for electron emission and energy loss, and in Sec. V we outline our conclusions. Atomic units are used unless otherwise stated.

II. THEORETICAL MODEL

When a heavy projectile impinges at grazing incidence on a solid surface, it interacts mainly with valence electrons belonging to the first atomic plane. For ionic crystals, as a consequence of the localized character of the valence orbitals [7], we can assume that electron emission from the surface is essentially caused by a sequence of binary collisions between the projectile and surface ions. Then the emission probability per unit path length from the initial state i bound to the surface is expressed as [3]

$$\frac{dP_i}{dx} = \delta_s \int_{-\infty}^{+\infty} dy\, P_i^{(at)}(\rho(\vec{r})), \tag{1}$$

where $P_i^{(at)}(\rho)$ is the probability of atomic ionization from the state i, as a function of the impact parameter ρ, and δ_s is the surface atomic density, which is considered a constant. In Eq. (1) the impact parameter ρ depends on the position $\vec{r}=(x,y)$ of the considered surface ion, with

$$\rho(\vec{r}) = \sqrt{y^2 + Z(x)^2}, \tag{2}$$

$Z(x)$ being the distance of the projectile to the surface, and x (y) the coordinate parallel (perpendicular) to the scattering

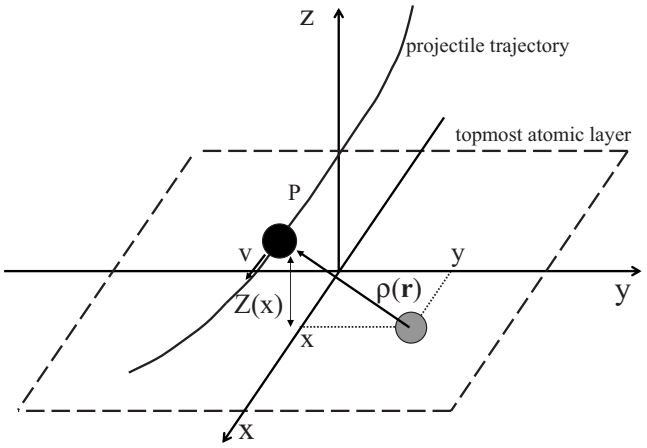

FIG. 1. Sketch of the coordinate system.

plane within the surface (see Fig. 1). Note that, unlike the differential atomic ionization probability, which describes the angular distribution of emitted electrons, the total probability of atomic ionization from the state i, $P_i^{(at)}$, does not depend on the azimuthal angle of the impact parameter, as results from Eq. (1).

In order to produce a consistent description of continuum electronic states in the fields of both the passing projectile and the effective charge left in the surface after ionization, we employ for the calculation of $P_i^{(at)}$ the CDW-EIS approximation. Within this theory the T-matrix element reads

$$T_{if} = \langle \chi_f^{CDW-} | W_f^{\dagger} | \chi_i^{E+} \rangle, \tag{3}$$

where χ_f^{CDW-} and χ_i^{E+} are the CDW and eikonal wave functions, with the proper asymptotic conditions in the final and initial channels, respectively, and W_f is the final perturbative potential. Details of the calculations can been found in previous papers [3,8].

In these collisions, apart from direct electron emission from the surface, there is another contribution from H^0 ionization (electron loss), which is at least one order of magnitude smaller. We have checked this by explicitly including electron capture and loss by the projectile. For the capture process we use the eikonal-impulse approximation, which is a distorted-wave method making use of the exact impulse and eikonal wave functions in the final and initial channels, respectively [9,10]. The projectile emission probability is calculated [6,11] in the impact-parameter first-Born approximation [12]. In this manner the charge state of the projectile along the trajectory is evaluated [6].

III. EXPERIMENTAL METHOD

The experiments are performed with a small ion accelerator at Humboldt University Berlin. Neutral hydrogen atoms with energies from 100 to 300 keV are scattered under grazing angles of incidence ranging from $\Phi_{in}=0.5°-1°$ from clean and flat LiF(001) and KI(001) surfaces. The target surface was kept under UHV condition at a pressure of typically some 10^{-11} mbar and prepared by frequent cycles of sputtering with 50 keV Ar ions under $\Phi_{in}=2°$ and subsequent annealing at 400 °C. The state of preparation of the target was checked via angular distributions of the scattered projectiles, which allows one to obtain information on the defect structure of the surface [13]. In the final state of preparation of the target, we observed well-defined angular distributions with negligible sub- and supraspecular tails which can be attributed to a mean width of terraces formed by the topmost layer atoms larger than 1000 a.u. In order to avoid macroscopic charging up of the target surface, the crystal was kept at a temperature between 100 and 300 °C, where alkali halide crystals show sufficient conductivity. By sets of horizontal and vertical slits the incoming proton beam was collimated to a divergence in the submilliradian domain and chopped by a pair of electric plates biased with voltage pulses with a rise time of a few nanoseconds. The pulsed ion beam was then neutralized via near-resonant charge exchange in a gas target operated with Kr atoms.

Since grazing scattering of atomic particles from the surface proceeds in the regime of surface channeling [13,14], the kinetic energy for the motion normal to the surface plane scales according to $E_\perp = E \sin^2 \Phi_{in}$. Then, for projectile energies of typically 100 keV, $E_\perp$ is in the eV range, so that projectiles cannot penetrate the bulk of the crystal and are specularly reflected from the topmost layer of surface atoms. The scattered beam is detected 1.38 m behind the target by means of a multichannel plate detector where the output pulse serves as start signal of a time-of-flight (TOF) setup for measurements of the projectile energy loss. The overall time resolution of our TOF system is about 5 ns, which amounts to an energy width of the scattered beam of about 1 keV at 100 keV impact energy.

The number of emitted electrons during the impact of a projectile is measured using a surface barrier detector (SBD) biased to a voltage of about 25 keV. The detector pulse height is proportional to the electron number ejected per projectile impact on the surface [15]. Emitted electrons are collected by a bias of some 10 V applied to a highly transparent grid, which also shields the target region from the high electric field owing to the high voltage on the SBD. As detailed elsewhere [16], coincident detection of projectile energy loss with the number of emitted electrons is achieved by relating the TOF signals to the pulse heights of the SBD. From the intensities of the SBD spectra for emission of a number of i electrons, W_i, we obtain the total electron yield $\gamma = \Sigma i W_i / \Sigma W_i$. Since the collection efficiency of our setup for emitted electrons is about 98%, accurate total electron yields are obtained by this method which can be compared to calculations on an absolute scale.

As an example for our experimental data we show in Fig. 2 the pulse height distributions of the amplified SBD signal for coincident (full circles) and noncoincident (open circles) detection with 100 keV H^0 projectiles specularly reflected from a LiF(001) surface under $\Phi_{in}=0.57°$. The pulse height scale of the SBD is converted to the number of emitted electrons, where the conversion factor is derived from previous experiments at lower projectile energies. Compared to the detection of low electron numbers, peaks owing to the emission of specific numbers of electrons are no longer resolved. The data show a Gaussian type of distribution peaking at

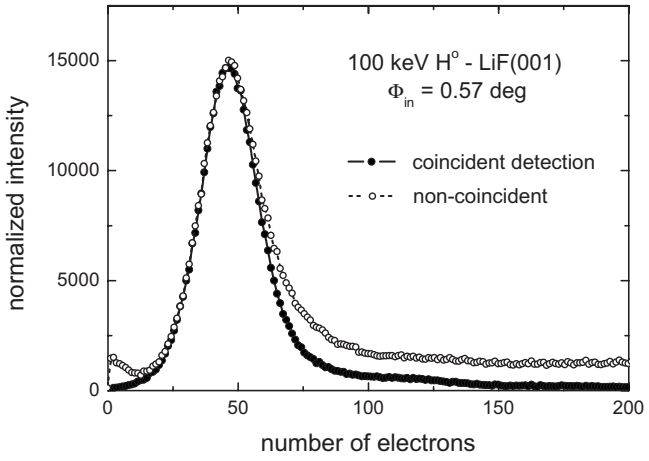

FIG. 2. Pulse height distributions of the amplified SBD signal for coincident (full circles) and noncoincident (open circles) detection with 100 keV H^0 projectiles specularly reflected from a LiF(001) surface under $\Phi_{in}=0.57°$.

about 50 emitted electrons. For the noncoincident detection of electrons we note additional signals owing to detector noise for low pulse heights and owing to subsurface scattering for higher pulse heights. The latter contribution to the noncoincident electron spectrum can be attributed to the penetration of projectiles into the subsurface regime, where electron densities are higher and, in particular, projectile trajectories for the interaction with the solid are much longer than for reflection in front of the surface plane [1]. The two spectra in Fig. 2 indicate that the present experimental method allows us to separate the two mechanisms for the kinetic emission of electrons from the target. We note that the frequently used technique based on measurements of target currents cannot be applied here because of these specific problems. Furthermore, charging-up effects present with insulators can be neglected here, since at a slightly elevated temperature (about 100 °C) the conductivity of LiF and KI is sufficiently high and the primary neutral beams consist of some 1000 atoms per second only (equivalent to ion currents of subfemtoampers).

IV. RESULTS

In the present work we studied grazing collisions of protons with LiF(001), KCl(001) and KI(001) surfaces in the intermediate- and high-velocity regime, i.e., impact energies ranging from 100 to 300 keV. For the different collision systems, we evaluated the charge state of the incident projectile along its trajectory and found that, even for the lowest energy, the fraction of protons is more than one order of magnitude greater than that of neutral hydrogen atoms [6]. This holds also for impact of neutral atoms, as follows from the calculations displayed in the lower panel of Fig. 3. Furthermore, the electron emission yield and energy loss due to projectile ionization for H^0-surface collisions are typically about one order of magnitude smaller than the contributions for the H^+-surface system. Therefore, direct ionization from the surface induced by bare ions is the dominating mecha-

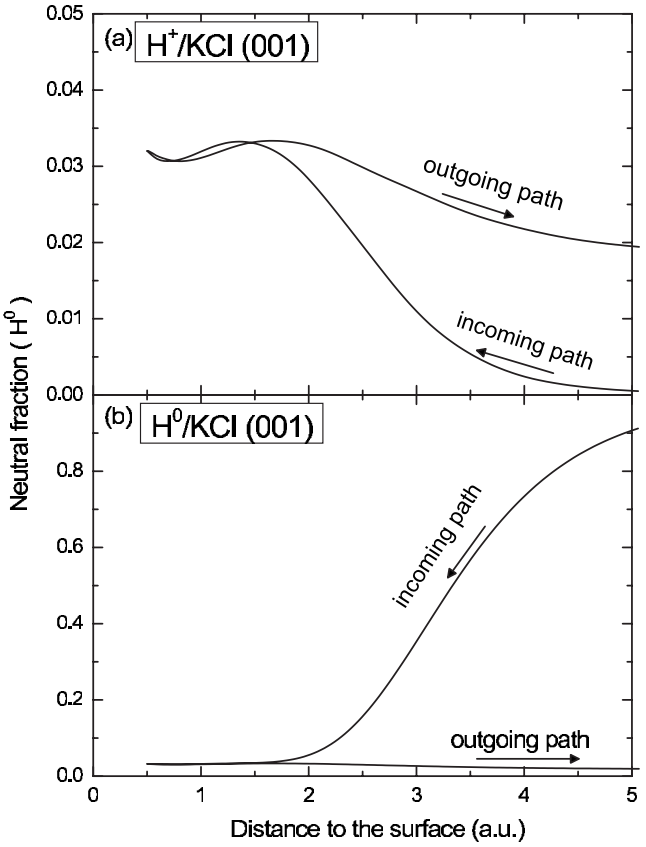

FIG. 3. H^0 fraction as a function of the distance of the projectile to the KCl(001) surface for incidence of 100 keV (a) protons; (b) neutral hydrogen atoms.

nism for the electron emission and energy loss of the projectile.

Owing to the geometry of the collision, associated with grazing trajectories, most emitted electrons come from outer shells of target ions. We consider the ionization from the *L*, *M*, and *O* shells of the F^-, Cl^-, and I^- anions, and from the *K* and *M* shells of the Li^+ and K^+ cations, respectively. In the evaluation of the atomic transition probability we used the Hartree-Fock wave functions of Ref. [17] to represent the initial atomic bound states, while the final continuum states, associated with electrons ejected from surface ions, were described as Coulomb wave functions with effective charges satisfying the corresponding initial binding energies.

The electron emission probability, which coincides with the average number of emitted electrons per incident ion, is obtained from Eq. (1) by integrating dP_i/dx along the projectile trajectory. To represent the classical path of the proton we employ the punctual model of Ref. [5], in which the projectile-surface potential is expressed as a sum of individual potentials that describe the static interaction between the projectile and the crystal ions placed at the lattice sites [18]. The projectile trajectory was derived from classical dynamics by employing the Runge-Kutta method, taking into account four atomic layers of the solid. The polar angle of the incident velocity was chosen far from low-index crystallographic directions ($\theta_i=30°$), and for every angle Φ_{in} approximately 50 specularly reflected trajectories with random

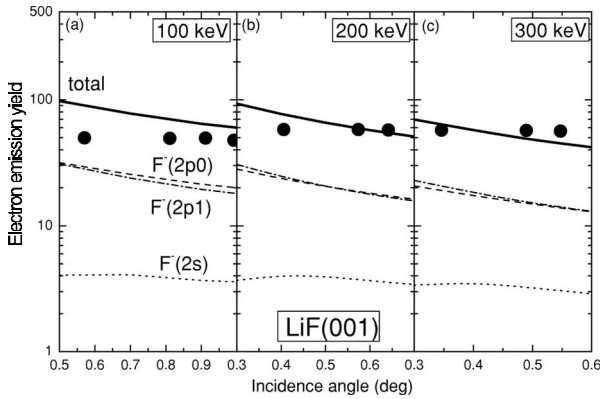

FIG. 4. Electron emission yields for grazing protons colliding with LiF(001) surfaces, as a function of the incidence angle, measured with respect to the surface plane. Three different impact energies are considered: (a) 100; (b) 200; (c) 300 keV. Full dots, present experimental data; solid lines, theoretical values derived as explained in the text.

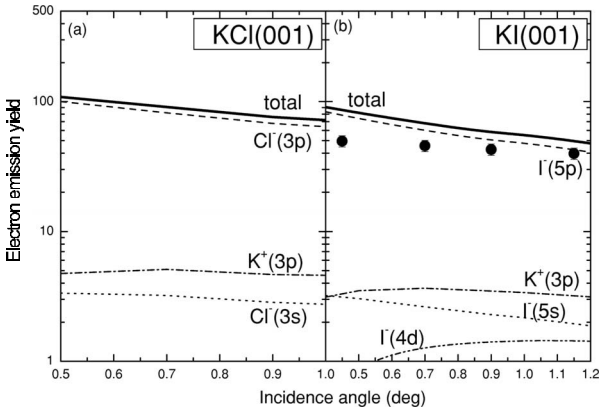

FIG. 5. Similar to Fig. 4 for 100 keV protons impinging on (a) KCl(001) and (b) KI(001) surfaces.

initial positions were considered. Note that, at the present impact energies, the long lifetime of the charge imbalance left on the surface by successive ionization produces a track of positive effective charges that might affect the proton trajectory [8]. However, this interaction is partially compensated by the dynamic polarization of the surface [18], which is weaker than for metal surfaces but acts for a long time in a grazing collision, so it may reduce the effect of the track potential.

A. Electron emission

We start the analysis by a discussion of electron emission from a LiF surface and a comparison of our calculations with the experimental data. In Fig. 4 we display total electron emission yields, which are identical with total electron emission probabilities, as a function of the incidence angle for three different impact energies: 100 (left panel), 200 (middle panel), and 300 keV (right panel). The theoretical results are compared with measurements where via a bias potential of some 10 V electrons are collected with a detection efficiency close to 1. Our calculations show an overall accord with the experiments; as expected for a first-order distorted-wave theory, the agreement improves when the impact velocity increases. Note, however, that in spite of the general concordance between theory and experiment, measurements do not vary appreciably with the incidence angle and energy, while theoretical values show a slight decrease as these parameters increase. In our calculations the dominant process corresponds to emission from $F^-(2p)$ orbitals and the contribution from Li^+ (not displayed in Fig. 4) is around two orders of magnitude lower than that from F^- due to the small radius of the alkali-metal ion. With respect to the projectile path, note that the critical angle at which the projectile penetrates in the solid is very sensitive to the projectile-surface potential. As an example, for 100 keV proton impact with an incidence angle $\Phi_{in}=1°$, within the punctual model only 4% of the trajectories are specularly reflected at the topmost atomic layer. For such reflected trajectories the projectile moves very close to the surface plane, producing a large electron emission yield. We have also investigated the effect of the polarization potential proposed in Ref. [18]. Even though at large incidence angles the polarization considerably affects the penetration of ions, under specular reflection conditions its effect on our theoretical results was found to be small.

In Fig. 5 we show electron emission probabilities for 100 keV protons impinging on two different targets, KCl(001) (left panel) and KI(001) (right panel). Again the outer p orbitals of the target anions give the most important contribution to electron emission, while contributions to electron yields from K^+ cations are substantially smaller. Measurements of electron emission yields for a KI(001) surface are displayed in Fig. 5(b). As also observed in Fig. 4(a), at 100 keV the present distorted-wave theory overestimates the experimental data for small incidence angles, tending to the measured values as Φ_{in} increases. By comparing Figs. 4(a) and 5 we reveal that the electron emission probability varies only slightly with the crystal surface. For a given glancing incidence angle, the theoretical electron emission yields are comparable for the three targets considered. This can be associated with the fact that two related effects almost compensate each other: a larger surface ion radius gives rise to a higher probability of atomic ionization for surface atoms, but also to a lower surface atomic density, which leads to a lower emission probability from the surface.

In all cases, our results show a high efficiency of light projectiles like H^+ in ionizing the surface of ionic crystals, producing more than 50 ionizations on the average for 100–300 keV. This yield is clearly larger than the number of emitted electrons from, e.g., a Cu surface for similar impact velocities [19]. In general, total electron emission yields from insulator surfaces are substantially higher than those from metal or semiconductor surfaces [1,20].

B. Energy loss

The loss of kinetic energy suffered by the projectile during the collision with the surface is associated with the energy transferred in electronic transitions. We evaluate the energy lost by the projectile from Eq. (1) by replacing the

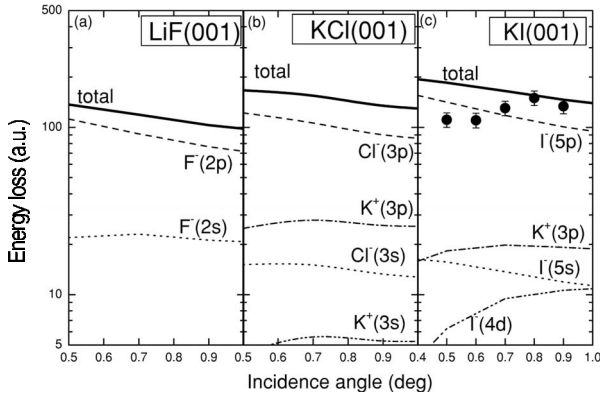

FIG. 6. Energy loss for grazing scattering of 100 keV protons from insulator surfaces, as a function of the incidence angle. The target surfaces are (a) LiF(001), (b) KCl(001), and (c) KI(001). Solid lines, theoretical results; full dots, present experimental data.

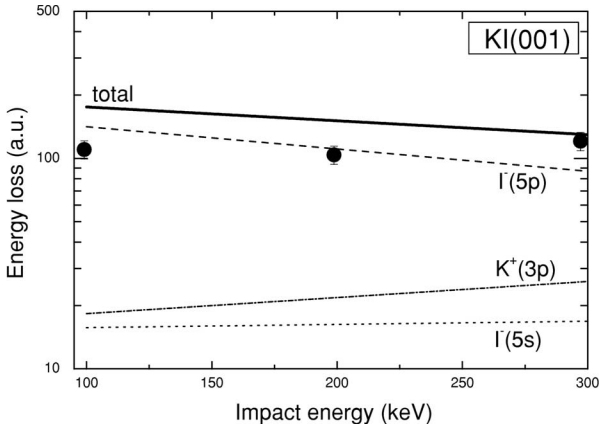

FIG. 7. Energy loss for grazing scattering of H^0 from KI(001) surfaces, as a function of the impact energy. Full dots, present experimental data; solid line, theoretical results for proton impact.

atomic transition probability by the energy loss corresponding to the atomic ionization process [8].

Theoretical energy losses for 100 keV protons impinging on LiF (left panel), KCl (middle panel), and KI surfaces (right panel) are displayed in Fig. 6 as a function of the incidence angle. Measurements for KI are also included in Fig. 6(c). Again, at 100 keV impact energy the theoretical values agree with the experiment for large incidence angles, running above measured data for $\Phi_{in} \lessapprox 0.7°$. For KCl and KI, in contrast to electron emission, contributions to energy loss from $K^+(3p)$ orbitals become relevant, and the importance decreases only as the incidence angle is reduced. For LiF, instead, the energy lost by the projectile in collisions with alkali-metal ions is more than one order of magnitude lower than the anion contribution. This holds also for large incidence angles for which the projectile probes the region close to the surface.

In Fig. 7 we display the energy loss of neutral hydrogen atoms impinging on a KI(001) surface with a glancing angle ($\theta_i = 0.5°$). Measurements of the energy loss as a function of the incidence energy are compared with theoretical results derived from our model by considering proton impact. At high energies the projectile moves close to the surface mostly as a bare ion. This holds also for incidence of H^0 projectiles (cf. Fig. 3). Theoretical and experimental values are in a good agreement, showing only a slight overestimation of the experimental data at lower energies. As pointed out before, this discrepancy might be based on the first-order perturbative approach used here [21].

V. CONCLUSIONS

We have presented calculations for the emission of electrons from LiF, KCl, and KI crystal surfaces by grazing incidence of H^+, and measurements for electron emission from LiF and KI surfaces by impact of H^0 projectiles. We showed that the main mechanism of electron emission is the direct ionization of the surface induced by protons. Contributions to electron emission from the H^0 charge state of the projectile were found negligible since this charge fraction is an order of magnitude smaller than the H^+ fraction at the energies considered here. For the different crystals, theoretical predictions show a weak dependence on the surface density because the effect of a smaller surface density for a larger halogen ion radius is compensated by a larger ionization cross section.

Reasonable agreement between theoretical and experimental data was found. The theory reproduces well measured values for high impact energies, departing from the experimental results when both incidence energy and angle decrease. Total electron emission yields amount to about 50 electrons for 100–300 keV protons impinging on a LiF surface. These values are larger than those observed for metal or semiconductor surfaces [1,19].

The energy loss of projectiles along the grazing trajectory was also investigated, analyzing the contributions from different subshells of the target ions. Theoretical values were compared with experimental data for H^0 projectiles colliding with KI surfaces, and a fairly good concordance between them was found. As in the case of electron emission, measurements are almost independent of the impact velocity, while calculations smoothly decrease with the increase of this parameter, showing a better accord with the experiment for high velocities.

ACKNOWLEDGMENTS

This work was supported by CONICET, UBA, and ANPCyT of Argentina and by the DFG under Contract No Wi1336. M.S.G. thanks the High-Performance Opteron Parallel Ensemble Cluster (Institute of Astronomy and Space Science) for providing computational support for this work. I.A. and A.A. are grateful to the Basque Departamento de Educación, Universidades e Investigación, the University of the Basque Country UPV/EHU, the Spanish Ministerio de Educación y Ciencia, and the EU Network of Excellence NANOQUANTA (Grant No. NMP4-CT-2004-500198) for financial support.

[1] K. Kimura, G. Andou, and K. Nakajima, Phys. Rev. Lett. **81**, 5438 (1998).
[2] H. Winter, Prog. Surf. Sci. **63**, 177 (2000).
[3] M. S. Gravielle, Phys. Rev. A **62**, 062903 (2000).
[4] P. D. Fainstein, V. H. Ponce and R. D. Rivarola, J. Phys. B **24**, 3091 (1991).
[5] A. J. García and J. E. Miraglia, Phys. Rev. A **74**, 012902 (2006).
[6] I. Aldazabal, M. S. Gravielle, J. E. Miraglia, A. Arnau, and V. H. Ponce, Nucl. Instrum. Methods Phys. Res. B **232**, 53 (2005).
[7] A. Zunger and A. J. Freeman, Phys. Rev. B **16**, 2901 (1977).
[8] A. Arnau, M. S. Gravielle, J. E. Miraglia, and V. H. Ponce, Phys. Rev. A **67**, 062902 (2003).
[9] M. S. Gravielle and J. E. Miraglia, Phys. Rev. A **44**, 7299 (1991).
[10] M. S. Gravielle and J. E. Miraglia, Phys. Rev. A **51**, 2131 (1995).
[11] I. Aldazabal, V. H. Ponce and A. Arnau, Phys. Status Solidi B **241**, 2374 (2004).
[12] M. R. C. McDowell and J. P. Coleman, *Introduction to the Theory of Ion-Atom Collisions* (North-Holland, Amsterdam, 1970).
[13] H. Winter, Phys. Rep. **367**, 387 (2002).
[14] D. S. Gemmell, Rev. Mod. Phys. **46**, 129 (1974).
[15] F. Aumayr, G. Lakits, and HP. Winter, Appl. Surf. Sci. **63**, 177 (1999).
[16] A. Mertens *et al.*, Nucl. Instrum. Methods Phys. Res. B **182**, 23 (2001).
[17] E. Clementi and C. Roetti, At. Data Nucl. Data Tables **14**, 177 (1974), Tables 2 and 44.
[18] A. J. García and J. E. Miraglia, Phys. Rev. A **75**, 042904 (2007).
[19] S. Lederer and H. Winter, Phys. Rev. A **73**, 054901 (2006).
[20] M. Vana, F. Aumayr, P. Varga, H. P. Winter, Europhys. Lett. **29**, 55 (1995).
[21] P. D. Fainstein, V. H. Ponce, and A. E. Martinez, Phys. Rev. A **47**, 3055 (1993).